SLAC-PUB-14675

BUNCH LENGTH AND IMPEDANCE MEASUREMENTS AT SPEAR3*

Jeff Corbett#, Weixing Cheng, Alan S. Fisher and Xiaobiao Huang
Stanford Linear Accelerator Center, 2575 Sand Hill Road, Menlo Park, CA 94025

Abstract

Streak camera measurements were made at SPEAR3 to characterize longitudinal coupling impedance. For the nominal optics, data was taken at three rf voltages and a single-bunch current range of 0-20mA. Both bunch-centroid phase shift and bunch lengthening were recorded to extract values for resistive and reactive impedance. An (R+L) and a Q=1 model were then back-substituted into the Haissinski equation and compared with raw profile data. In the short bunch (low-α) mode, distribution 'bursting' was observed.

INTRODUCTION

SPEAR3 is a 3 GeV light source with a relatively smooth Cu vacuum chamber and four PEP-II style mode-damped RF cavities. The storage ring presently contains 9 insertion devices with carefully tapered transitions and in some cases copper-plated ID chambers. As a result, the storage ring has a low longitudinal coupling impedance. Interestingly, due to the large number of dipole magnets (36 total), the momentum compaction is small and the natural bunch length is of order 20 ps rms (6mm). Although the classical 'long bunch' approximations are suspect in this regime, we nevertheless apply Zotter's formula for potential-well distortion [1].

In the low-α mode, the bunch length is reduced to only a few ps (<1mm) and Zotter's PWD formula no longer holds. Instead, consistent with theory and observation at other laboratories [2,3] we see rapid CSR-induced bunch lengthening starting from very low currents. As outlined below, in the $\alpha_o/21$ configuration we also see bursting with streak and gated camera measurements.

In each case data was acquired using green light on the SPEAR3 diagnostic beam line [4]. The primary diagnostics are a Hamamatsu C5680 streak camera and a fast-gated Roper/PiMax camera.

BROADBAND COUPLING IMPEDANCE

The longitudinal broadband coupling impedance of a storage ring can be summarized using overlap integrals between the point-charge impedance of the storage ring Z(ω) and the power spectrum of a single bunch. The resulting real (resistive) and imaginary (reactive) components of the overlap integrals are referred to as 'effective' because they express complicated frequency-dependent beam/ring interactions as compact scalar values. Although understanding the precise shape of Z(ω) is difficult, we can nonetheless measure values for $\mathrm{Re}\{Z_{\|}^{eff}/n\}$ and $\mathrm{Im}\{Z_{\|}^{eff}/n\}$ experimentally and construct macroscopic equivalent-circuit models based on the result.

In this paper we first extract the resistive component 'R' (loss factor) from synchronous-phase shift measurements and the inductive component 'L' from bunch lengthening measurements at three different rf voltages. We then back-substitute the 2-parameter resistor/inductor models into the Haissinski equation to test for self-consistency. A 3-parameter, Q=1 model is also tested both with the Haissinski equation and in terms of effective impedance predicted by the overlap integrals.

Resistive Impedance

The synchronous phase ϕ_s is the result of total average power loss including SR radiation and chamber impedance. With sufficiently high overvoltage, the bunch rides to good approximation on the linear portion of the rf waveform and the loss factor (V/pC) can be determined by measuring phase shift as a function of single bunch current. Figure 1 shows the raw phase shift data and linear trend curves at V_{RF}=2.4MV, 2.8MV and 3.2MV. The phase-shift was measured in synchroscan mode by monitoring the change in pulse arrival time between 0.1mA reference bunches and a test bunch.

The resulting loss factors $k_{\|} = V_{RF}\cos(\phi_s)\Delta\phi_s(1/Q_b)$ are listed in Table 1. As expected, short bunches have larger loss factors. In the frequency domain this is consistent with increased overlap between the resistive broadband impedance and the widening single-bunch power spectrum. The resistive impedance also causes current profile asymmetry (see Figures 3,4). The equivalent frequency-independent, Gaussian-bunch resistance calculated from $R = 2\sqrt{\pi}\sigma k_{\|}$ is also shown in Table 1.

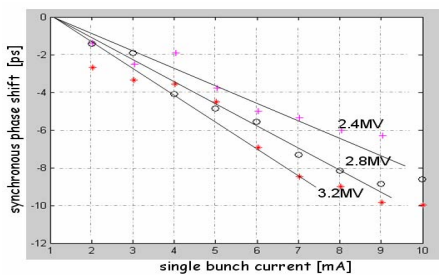

Figure 1: $\Delta\phi_s$ versus single-bunch current for RF voltages 2.4MV, 2.8MV and 3.2MV.

* Work sponsored by U.S. Department of Energy Contract DE-AC03-76SF00515 and Office of Basic Energy Sciences, Division of Chemical Sciences.
# corbett@slac.stanford.edu

Reactive Impedance

The inductive component of the reactive impedance leads to potential-well distortion and consequently tune shift and bunch lengthening. The *effective* reactance is again an overlap integral between the point-particle impedance Z(ω) and the bunch spectra†. Like most storage rings SPEAR3 is predominantly inductive and the reactive impedance increases with bunch length.

To calculate the $\mathrm{Im}\{(Z/n)_{eff}\}$ values in Table 1 we applied Zotter's formula for potential-well distortion [1]

$$\left(\frac{\sigma_z}{\sigma_{z0}}\right)^3 - \frac{\sigma_z}{\sigma_{z0}} = \frac{1}{\sqrt{2\pi}} \frac{\alpha_c e I_b}{E_0 \nu_{s0}^2} \left(\frac{c}{\omega_{\mathrm{rev}} \sigma_{z0}}\right)^3 \mathrm{Im}\left[\left(\frac{Z}{n}\right)_{\mathrm{eff}}\right] \quad (2)$$

where E_0 is the beam energy, ν_{s0} is the synchrotron tune and ω_{rev} is the revolution frequency. The corresponding values for effective inductance $L_{eff}\,\omega_{rev} = \mathrm{Im}\{(Z/n)_{eff}\}$ are also listed in Table 1. The natural bunch length, σ_{zo} scales closely with $\sqrt{V_{rf}}$.

Table 1: Natural bunch length, loss factor and impedance values for SPEAR3. 'Z/n' refers to the reactive component (effective) computed using Eq. 2. Row 4 refers to achromatic optics, lower momentum compaction.

V_{rf}[MV]	σ_o [ps]	k [V/pC]	R [Ω]	Z/n [Ω]	L [nH]
3.2	20.8	9.3	646	0.19	23.6
2.8	22.3	7.7	572	0.20	24.9
2.4	24.7	5.3	432	0.21	27.4
3.2 AC	16.6	-	-	0.17	21.1

Impedance Models

As a test of the R+L coupling impedance model [5] we back-substituted the measured values into Haissinski's equation [6] to solve for the equilibrium current distribution as a function of bunch current and compared with the raw data. In this case, the induced voltage is simply V_{ind}=RI+ LdI/dt. Figure 3 shows the results for the 2.4MV, 2.8MV and 3.2MV accelerating voltage data. Clearly the calculation does not match well with the raw data at higher currents. It appears with shorter bunches there is higher energy loss corresponding to more resistive impedance than predicted. Similarly, the low inductive impedance is not explained by the R+L model.

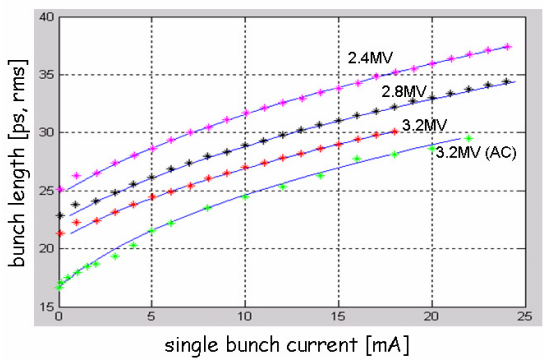

Figure 2: Bunch length and fit as a function of current for three rf voltages. Bottom curve is achromatic optics.

† Reference [1] describes the proper choice of the bunch power spectra needed to calculate $\mathrm{Im}\{(Z/n)_{eff}\}$

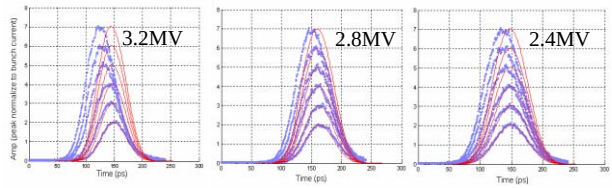

Figure 3: Haissinski curves for R+L model. Blue dots are raw data, solid red curves are fitted result.

To improve the agreement we used a Q=0.7 resonant-impedance model with center frequency f_r=30GHz and a shunt impedance R_s=10kΩ. Figure 4 shows the comparison of the self-consistent profile calculations using the Q=0.7 resonant model with the raw data up to 7ma/bunch. The improved agreement comes from both the frequency-dependence of the resistive component and the added capacitive component of the reactive component at higher frequencies.

If we evaluate the overlap integrals for effective impedance, the Q=0.7 model produces good agreement for the resistive component but the reactive component is about a factor of 2 higher than predicted using Eq. 2. The results for this model are shown in Table 2 where 'R' has been evaluated using $R = \mathrm{Re}\{Z_{\parallel}^{eff}/n\} * \sigma\omega_{rev}$ [7]. The higher inductance values may be due to the fact that in SPEAR3 σ_z<<b, ie, Eq. 2 may not suitable for such short bunches.

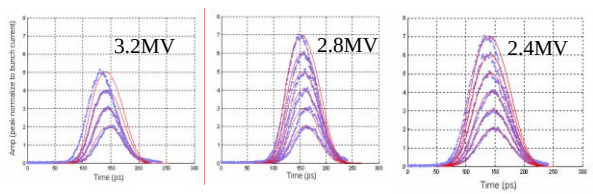

Figure 4: Haissinski curves for Q=0.7 model. Blue dots are raw data, solid red curves are fitted result.

Table 2: Effective impedance from broadband resonator model (Q=0.7, R_s=10kOhm, f_r = 30GHz)

	measured			calculated		
σ_o [ps]	K [V/pC]	R [Ω]	Im[Z/n]	K [V/pC]	R [Ω]	Im[Z/n]
20.8	9.3	646	0.19	9.2	820	0.47
22.3	7.7	572	0.20	7.5	753	0.49
24.7	5.3	432	0.21	5.6	560	0.51

LOW-α BUNCH BURSTING

The ultra-fast science program at SSRL includes development of short, ps-range x-ray pulses using the SPEAR3 beam. Scaling by $\sqrt{\alpha}$ (momentum compaction) requires a modest reduction in α of order 20-500. To date, lattices have been tested with α_0/21, α_0/59, α_0/340 with

natural bunch lengths of σ_0=3.7, 2.2, 0.9ps rms [8]. As reported in [9], experimental determination of the natural bunch length is limited by system resolution and the low-α bunch length increases rapidly with current [10].

In subsequent tests, the rf voltage was lowered to accumulate up to 7ma in a single, ~20ps (rms) bunch. With the $\alpha_0/21$ lattice, clear signatures of quasi-periodic 'bursting' were observed with the streak camera in dual-sweep mode (Fig. 5). The sawtooth bursting has a period of ~6ms (2-3 damping times). Signatures of bursting had been observed previously on an IR bolometer [10].

With time moving left to right, the image can be interpreted as consisting of slow periods when charge coalesces to the bunch core followed by a rapid 'burst' and loss of photons within the camera field of view. The bursts are visible in the light-blue 'neck' regions of Fig. 5a. Gaussian fitting indicates the pulse length does not change appreciably during the process (Fig. 5b). Bursting persists for RF voltages ranging from the nominal value of 3.2MV down to less than 1.3MV and the period changes with current Bursting was not visible at high single-bunch current in either the $\alpha_0/59$ or $\alpha_0/340$ lattices.

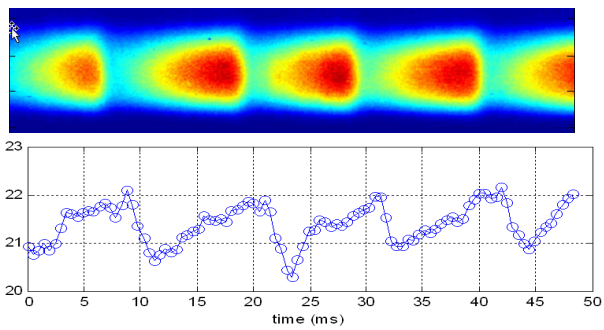

Figure 5: Dual-axis bursting in SPEAR3 at 5.3 mA with the $\alpha_0/21$ lattice. (a) Streak camera image. (b) Bunch length (ps, rms) extracted from image.

Following the premise that in the coalesced-state the bunch emits 'bursts' of CSR, we used the technique introduced in [11] with a 90° beam profile rotation, cylindrical lenses and a rotating mirror upstream of a fast-gated PiMax camera to measure time evolution of the transverse beam profile.

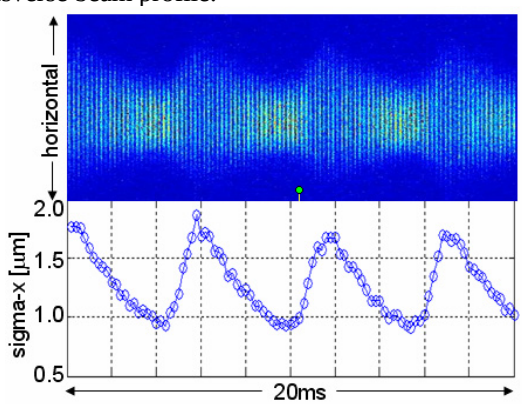

Figure 6: Single-turn images of single-bunch profile with bursting active in SPEAR3 low-alpha lattice.

Figure 6 shows the result for a sequence of images separated by 200μs. The bursting shows up as >50% increase in horizontal beam size from either emittance blow-up, increase in energy spread or both.

SUMMARY

Bunch-length and phase-shift measurements in SPEAR3 were used to evaluate the resistive (loss factor) and reactive (PWD) components of the longitudinal broadband impedance at three different rf voltages. Assuming a frequency-independent value for R and fitting Zotter's equation for L yields a two-parameter model with marginal performance when back-substituted into the Haissinski equation. A Q=0.7 model with center frequency 30GHz and 10kΩ shunt impedance produced better results but predicted higher values for $\mathrm{Im}\left\{(Z/n)_{eff}\right\}$. Quasi-periodic 'bursting' was observed with both streak- and fast-gated cameras at high single-bunch current in the $\alpha_0/21$ lattice.

ACKNOWLEDGEMENTS

We gratefully acknowledge the advice and assistance of K. Bane, E. Irish, W. Mok, J. Safranek, J. Sebek and the SPEAR3 operations staff.

REFERENCES

[1] B. Zotter, 'Potential-Well Bunch Lengthening', CERN SPS/81-14 (1981).
[2] G. Stupakov, et al, 'Beam Instability and Microbunching due to Coherent Synchrotron Radiation', Phys. Rev. ST Accel. Beams 5, 054402 (2002)
[3] J. Feikes, *et al*,'Sub-Piocsecond Electron Bunches in the BESSY Storage Ring', EPAC04, Lucerne, Switzerland (2004).
[4] J. Corbett, *et al*, 'The SPEAR3 Diagnostic Beamlines', PAC05, Knoxville, Tennessee, USA (2005).
[5] R. Holtzapple, *et al*, 'Single Bunch Longitudinal Measurements at the Cornell Electron-Positron Stroage Ring' Phys. Rev. ST Accel. Beams, 3:03441 (2000).
[6] J. Haissinski, 'Exact Longitudinal Equilibrium Distribution of Stored Electrons in the Presence of Self-Fields', Nuovo Cimento, Vol. 18B, No. 1 (1973).
[7] J. Bergstrom, private communication.
[8] X. Huang *et al*., 'Low-Alpha Mode for SPEAR3', PAC07, Albuquerque, NM, (2007).
[9] W. Cheng, A.S.Fisher and J. Corbett, 'Streak Camera Measurements in PEP-II and Variable Optics in SPEAR3', BIW08, Lake Tahoe, CA (2008).
[10] W.J. Corbett, *et al*., 'Bunch-Length Measurements in SPEAR3', PAC07, Albuquerque, NM (2007).
[11] A.S. Fisher, *et al.*, "Turn-by-Turn Imaging of the Transverse Beam Profile in PEP-II," BIW06, Batavia, IL, 1–4 May 2006, p. 303, SLAC-PUB-11851.